EFFECT OF PRODUCTION INDUCED POROSITY ON THE STRUCTURAL BEHAVIOUR AND DAMAGE ONSET IN NCF COMPOSITES

M. Scheerer[1*], V. Calard[1], T. Goss[1], P. Hahn[1], M. Henzel[1], Z. Simon[1]

[1]*Aerospace & Advanced Composites GmbH. Materials & Component Testhouse, 2444, Seibersdorf*
** Michael.scheerer@aac-research.at*

Keywords: Multi-Scale FEM Simulation, Infusion, Porosity, Acoustic Emission

Abstract
Infusion processes like RTM or vacuum infusion show high potential in the automated production of components made from fiber reinforced plastics. One critical issue is the "pore free" impregnation of the dry performs in order to guaranty the structural integrity. In this work the authors present simulation and experimental results on the quality of the production process and the mechanical behavior of composite plates made of $[-45/45]_{12s}$ *non-crimp fabrics (NCF) infiltrated by vacuum infusion with different flow aids leading to different void contents.*

1 Introduction
In order to bring the advantages of fiber reinforced polymers – high specific strength and stiffness – into markets like car industry where mass production is essential, automated manufacturing techniques have to replace the wide spread manual production. Depending on the part to be manufactured, infusion methods like Resin Transfer Molding (RTM) and Vacuum Infusion (VI) or automated fiber placements (AFP) are such automated production techniques [1]. Vacuum Infusion shows a high potential as it needs only one flexible membrane (e.g. polymer foil) on the mold and can be used in combination with AFP of dry performs. The most important step in the production of composite parts by resin infusion is to reach a full impregnation as the resin propagates between the fiber bundles and fibers. The impregnation driving force is usually resulting from pressure difference which is limited by VI to maximum of around 0.5 bar depending on the resin system [2]. Depending on the type and architecture of the dry pre-form – e.g. woven fabrics or non crimped fabrics [3] – inhomogeneous flow conditions within the mold during the infiltration can arise leading to the inclusion of pores that influence the structural behavior of the composite part. Simulation of the production process followed by structural analyses of the components with production induced imperfections - like pores - could strongly help the manufacturers in understanding the behavior of real – imperfect - composite parts.

2 MANUFACTURING OF PANELS BY VACUUM INFUSION
2.1 Materials
The materials used in this study were an infusion resin type Hexion Epikure L20 with hardener Hexion Epikote 960 and carbon fiber T700 preforms in non-crimp fabric (NCF) architecture. Prior to the production of the panels the required properties of resin system like

viscosity, curing kinetic, density, shrinkage and pot life have been measured. Out of this measurement an optimum temperature for infusion of 40°C was selected. At this temperature a maximum infusion time of approximately 1 hour could be achieved (limit of the viscosity to a maximum of 1 Pas). The selected reinforcement material was a T700 carbon fiber (diameter 7µm, 12K bundle) in a bi-diagonal nesting [-45/45] with Polyester sewing threads from SAERTEX (see Figure 1).

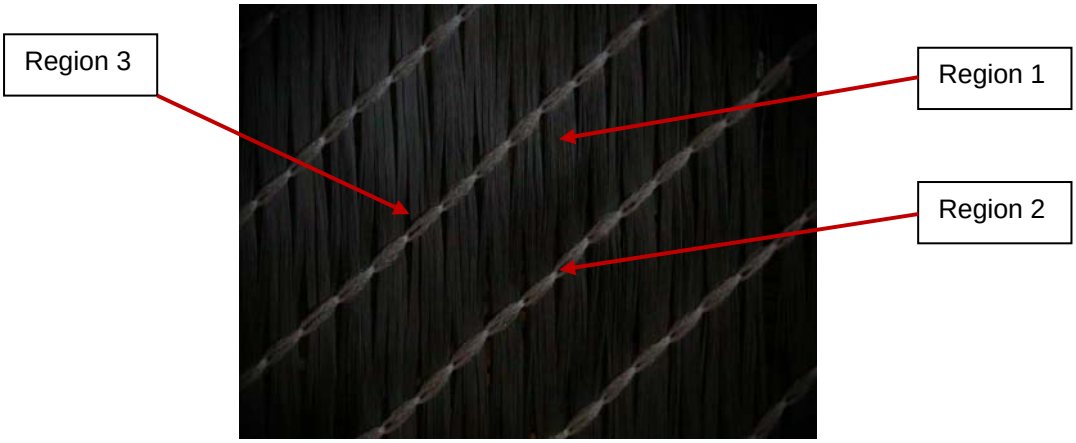

Figure 1. SAERTEX Bidiagonal-Carbon-nesting

The nesting shows three characteristic regions:

- region 1: the fibers are more or less aligned in the direction of the biaxial nesting (-45°/45°)
- region 2: Region of holes - sewing threads penetrate through both fiber layers – regions with pure resin after perfect infiltration
- elongated regions without fibers starting from region 2 – regions with pure resin after perfect infiltration

2.2 Description of the Infusion process

For the fabrication of the panels a standard infusion process using different types of flow aids have been used as shown schematically in Figure 2.

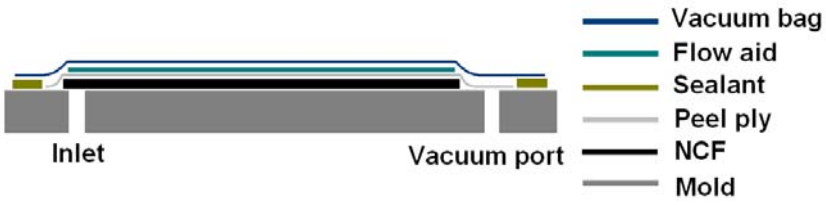

Figure 2. Schematic view of the vacuum infusion set-up

All plates have been produced on heat-able Al form. A line inlet and a point outlet were used. The supplied vacuum pressure during the infiltration was constant at p_{abs} = 0.4 bar. The following flow aids have been used: slow infiltration speed – no flow aid, medium infiltration speed – a breeder type Diatex PES340 and high infiltration speed – green flow from Airtech. After the infiltration the panels have been cured on the Al plate for typical cure cycles 4h at 60°C followed by 3h at 130°C (recommended cure cycle from the supplier). In addition a resin film infusion (RFI) process was used to produce reference panels with very low pore contents. In this process a thin resin film was placed on the dry perform and further molded by standard vacuum bag procedure. The infusion length was limited to the thickness of the

laminate. After the infusion the panel was placed in an autoclave and cured at a total pressure of 6 bar for 4 hours at 60°C followed by 4 hours of 130°C. After the production of the individual plates the quality of the panels (pore content) have been assessed by US inspection and by measuring the fiber and pore content according to ASTM D3171. Figure 3 illustrates the results from 3 typical panels with different pore contents.

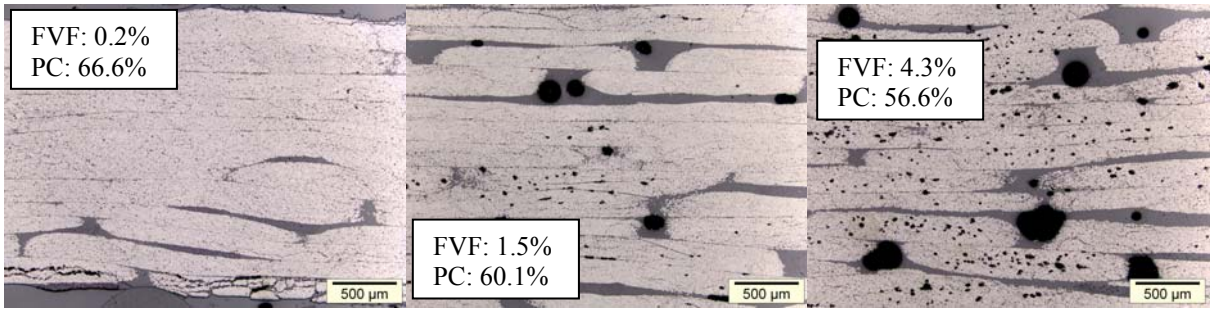

Figure 3. Fiber volume fraction (FVF) , pore content (PC) und micrographs of 3 typical panels produced with RFI and vacuum infusion with two different flow aids (left: RFI process, middle: no flow aid, right: green flow)

Out of the inspection one can conclude that the pore content increase and fiber volume fraction decrease with the infusion speed. Pores were observed in all three regions, where the largest nearly spherical shaped pores are located in region 2. In region 1 (region of the fibers) the pores are remarkable smaller.

3 Simulation Procedures

For the simulation of the infusion process and subsequent structural behavior of the cured structure it was divided in unit cells that were used for both simulations. In a first step the infusion process under the relevant boundary conditions at the border of the unit cell – including the effect of flow aids – were simulated by conventional FE software. The same unit cell was used to calculate the stiffness tensor, stress enhancement factors and inverse failure ratio for the used loading direction in ±45° to the fiber direction (based on Puck´s failure criterion) as function of the void content. In order to be able to compare the simulation results with experimental results on coupons a classical sub-modeling approach where the global model (coupon level) was used to assess the global deformations that act as boundary conditions for the unit cells, has been used to analyze the test.

3.1 Simulation of the Vacuum Infusion Process

The idealized 3D unit cell consist of 2 unidirectional layers one in 45° and the other in -45° orientation intersected by regions without fibers (regions 2 and 3) as shown in Figure 4.

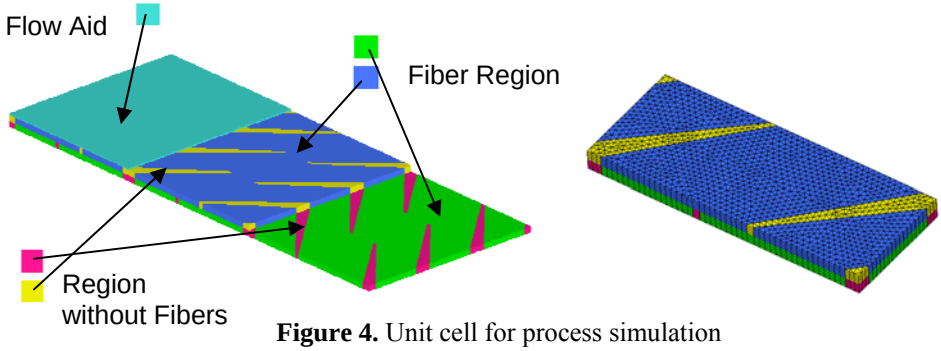

Figure 4. Unit cell for process simulation

In order to limit the influences from the boundaries, totally a matrix of 3 x 3 unit cells was used. Two different unit cells with and without flow aid were used in the analyses using the following parameters:

- Regions without fibers and flow aid: isotropic permeability of 10^{-9} m² / porosity = 1
- Regions with fibers: permeability of 10^{-12} m^2 parallel to the fibers und 10^{-13} m^2 perpendicular to the fiber direction / porosity = 0.3
- Pressure difference between inlet and vent: 0.6 bar

The following figure illustrates the propagating resin front during the infiltration with and without flow aid. Red regions represent infiltrated areas and blue regions illustrate dry areas.

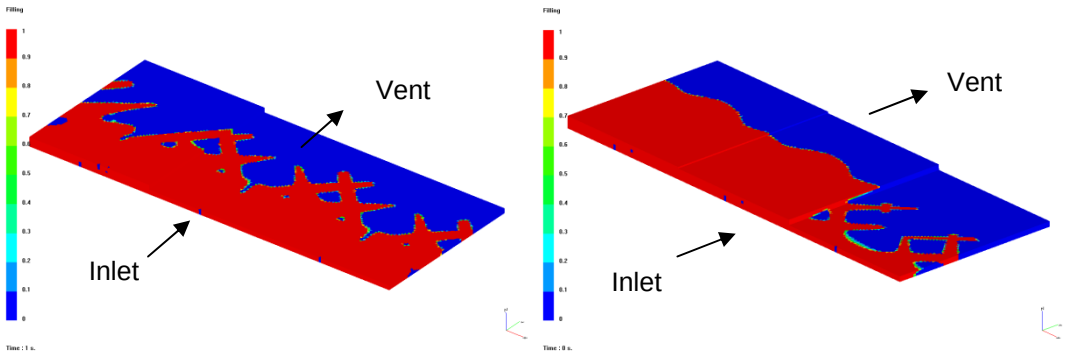

Figure 5. Flow front without flow aid (left) and with flow aid (right)

During the infiltration the resin propagated much quicker in the region without fibers leading to dry spots in the region of the fibers. Due to the higher flow speed in the flow aid this effect will be enlarged especially at the boundary to the flow aid. Therefore higher pore contents were observed in the simulation with flow aids. For the determination of the pore content only the inner unit cell of the 3 x 3 matrix was evaluated to represent proper boundary conditions (see Figure 6).

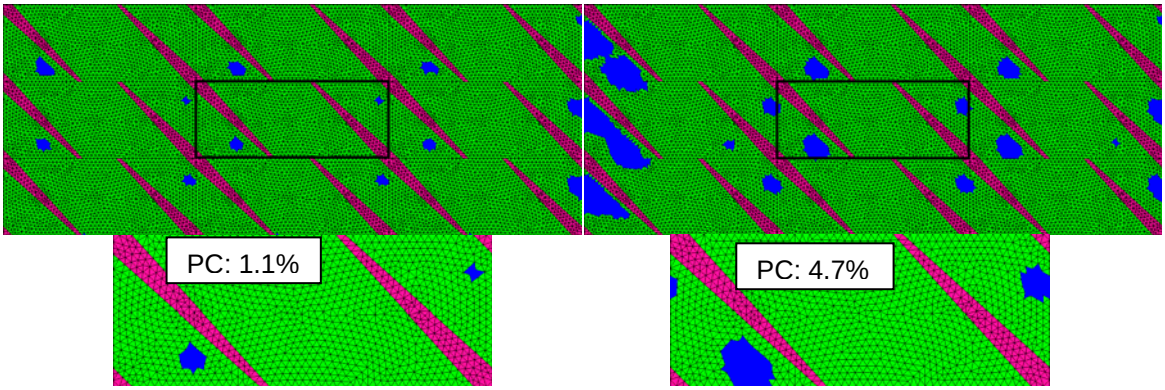

Figure 6. Distribution of the pores and pore content (PC) for two simulated infusion processes (left side: without flow aid – right side with flow aid)

The total pore content from the simulation is in very good agreement with the measured values, but the distribution of the pores differs clearly. In the simulation the pores appear only in the region of the fibers close to the region without fibers. The reason for that is that the used simulation software is not able to take into account capillary effects. The capillary forces act on the resin as long as it is liquid, tend to move the resin from regions with higher cavity to regions with lower cavity as the capillary pressure scales with 1/d where d is the

characteristic dimension of the cavity. Therefore the position of the pores moved toward the originally fiber free regions especially to the hole around the sewing threads as shown already in Figure 3. Due to that observation a direct transfer of the pores distribution to the unit cells used for the simulation of the mechanical behavior is not useful and an alternative approach described in the next chapter was used.

3.2 Simulation of the mechanical performance

As already mentioned in the previous chapter, the actual position of the pores cannot be derived from the process simulation model. Out of the micrographs shown in Figure 3 the pores exist in all 3 different regions of the unit cell of the NCF that representing two different materials with pores – pores within pure matrix and pores within the UD region. For the simulation of the mechanical behavior unit cells in three different length scales were used – the global model representing the test, a unit cell showing the characteristic of the NCF (same unit cell used for the process simulation) and 2 unit cells representing the pores in the matrix and in the UD material as shown in Figure 7.

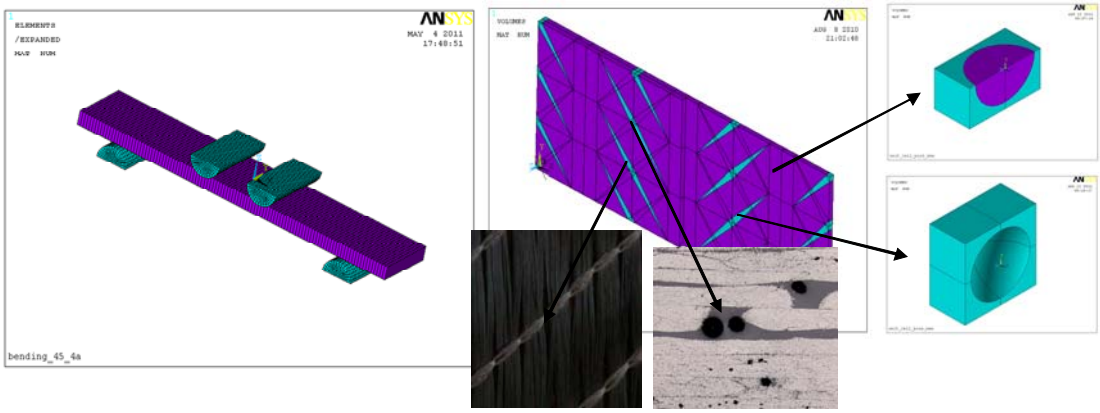

Figure 7. Used Unit cells for the simulation of the mechanical behavior

In a first step the two unit cells representing the pores were used to calculate the relative stiffness´s and inverse strength ratios ISR (based on Puck´s failure criterion [4]) as function of the pore content were different relative volumes between the pore and the surrounding materials have been used. The required transversal isotropic stiffness parameters for the UD region within the unit cell have been calculated out of standard micro-mechanical correlations and material data given in [4,5,6,7] assuming a constant fiber volume fraction of 65%. As the fibers only exist in the UD region of the NCF unit cell the total FVF of the unit cell was 60%.

Resin		UD – 65%				Inside pore in UD	
E [GPa]	3.2	$E_{\parallel}$ [GPa]	150.6	$R_{\parallel}$+ [MPA]	2591	$E_{\parallel}$ [GPa]	149.5
G [GPa]	1.2	$E_{\perp}$ [GPa]	10.97	$R_{\parallel}$- [MPa]	2137	$E_{\perp}$ [GPa]	0
R [MPa]	55	$G_{\perp\parallel}$ [GPa]	6.7	$R_{\perp}$+ [MPa]	70	$G_{\perp\parallel}$ [GPa]	0
T700 fiber		$G_{\perp\perp}$ [GPa]	4.1	$R_{\perp}$- [MPa]	240	$G_{\perp\perp}$ [GPa]	0
$E_{\parallel}$ [GPa]	230	$\nu_{\perp\parallel}$	0.272	R_{shear} [MPa]	105	$\nu_{\perp\parallel}$	0.33
$E_{\perp}$ [GPa]	13	$\nu_{\perp\perp}$	0.337			$\nu_{\perp\perp}$	0.5
$G_{\perp\parallel}$ [GPa]	50						
$\nu_{\perp\parallel}$	0.23						

Table 1: Material properties used for the simulation of the unit cells with pores – R: strength values

Figure 8 shows the calculated relative stiffness´s and relative inverse failure ratios for unit cells with pores in the matrix and UD regions.

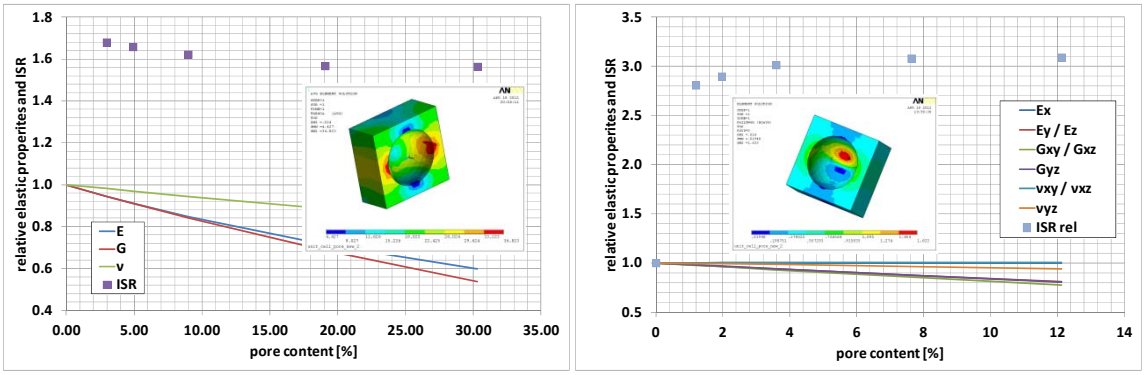

Figure 8. Calculated relative stiffness´s and relative inverse failure ratios for unit cells with pores in the matrix and UD regions

The stiffness´s decrease with increasing pore content. The relative ISR´s are remarkable higher for pores inside the UD region compared to pores in the pure matrix regions. Even at low pore contents the ISR is high and shows only a limited dependence on the pore content.
The relative stiffness´s were used as input parameters for the NCF unit cell to calculate the stiffness´s of the individual regions within the NCF unit cell as function of the fiber volume fraction and the pore content. In addition the relative ISR as function of the pore content were used to define new failure stresses under the relevant loading conditions (±45° relative to the fiber direction) as function of the pore content. Table 2 summarizes the calculated material parameters for pore contents of 0% and 5% in the resin region and in the UD region.

	UD region										
Pore content	$E_{\parallel}$	$E_{\perp}$	$G_{\perp\parallel}$	$G_{\perp\perp}$	$\nu_{\perp\parallel}$	$\nu_{\perp\perp}$	$R_{\parallel}+$	$R_{\parallel}-$	$R_{\perp}+$	$R_{\perp}-$	R_{shear}
[%]	[GPa]						[MPa]				
0	150.6	10.98	6.71	4.11	0.27	0.34	2591	2137	70	240	105
5	150.4	10.0	6.06	3.76	0.30	0.33	2591	2137	23	79	34
	Matrix region										
	E [GPA]		G [GPA]		ν		R [MPa]				
0	3.20		1.19		0.35		55				
5	2.91		1.08		0.34		33				

Table 2. Material properties used for the simulation of the NCF unit cell

These stiffness´s are used as input parameter for the global models – uni-axial tension and 4 point bending test in where the loading direction was ±45° relative to the fiber direction (dominant shear loading). The global model of the test (e.g. 4 point bending test as illustrated in Figure 7) was used to calculate the global deformation during the test. In order to analyze the local mechanical behavior the NCF unit cell was placed on the highest loaded regions within the global model where the global deformation out of the global model at the boundaries of the NCF unit cells act as boundary conditions for the NCF unit cell (classical sub-modeling approach). Using this approach the stresses at the level of the NCF unit cells were calculated and compared with the failure surfaces as function of the pore content derived from the unit cells with pores. Figure 9 shows the distribution of ISR (based on Puck´s failure criterion) over the NCF unit cell loaded with a nominal tension strain of 1% in y – direction for a component without pores, for a component with 5% pores in the matrix and 5% pores the matrix and the UD region.

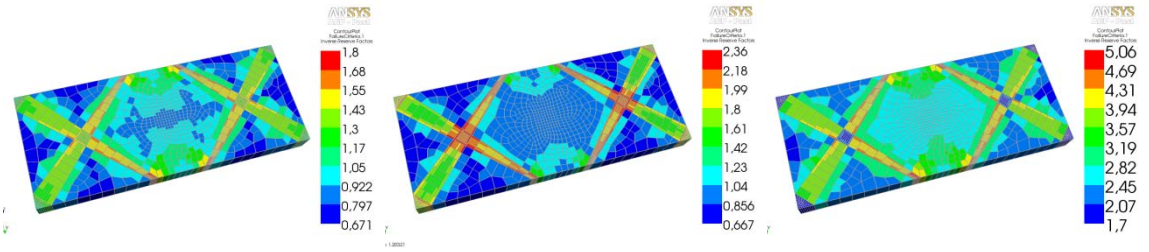

Figure 9. Distribution of ISR over the NCF unit cell loaded with a nominal tension strain of 1% in y – direction for a component without pores (left) for a component with 5% pores in the matrix (middle) and 5% pores in the matrix and the UD region (right)

If no pores are present in the structure the component will fail within the UD region close to the pure matrix regions by matrix tension. If the pores are only present in the resin region the component will fail within the resin region. If pores are present in both regions the failure starts in the UD region by matrix tension failure. These observations were similar for both tension and bending loading, where failure in bending occurred on the tension side. The ISR values were used to calculate the FPF stresses for both load cases – tension in y-direction and 4 point bending in z direction by dividing the nominal stress – measured also during the experiments – by the ISR value. Figure 10 shows the failure stresses for components with different pore contents in the matrix and the UD regions for both load cases.

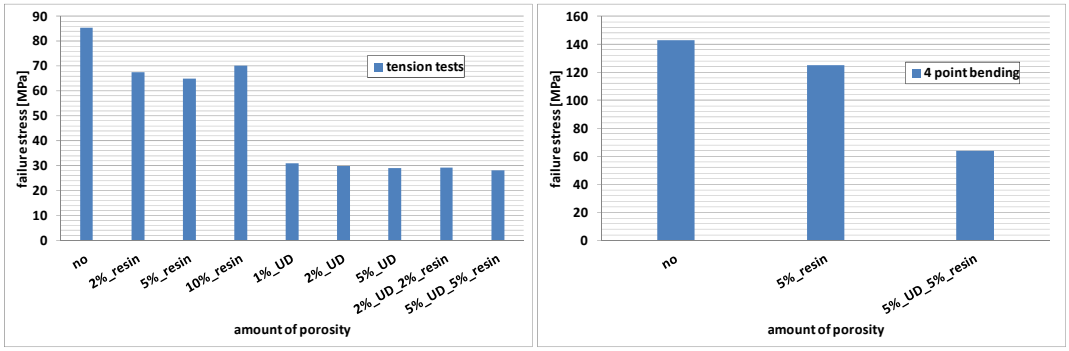

Figure 10. Failure stresses for components with different pore contents in the matrix region and the UD region for both load cases

Out of the simulation one can see that pores within the fiber region of the NCF show the largest effect on the damage onset. The reason for that can be found in the fact that the stiffness´s within the fiber region are remarkable higher compared to the resin regions leading to higher stress enhancement factors. The amount of pores (at least in the analyzed range between 1 and 10%) shows only limited effect on the onset of damages

5 Verification Tests with Online AE Monitoring

Tension and 4-point bending tests on ±45° specimen (relative to the dominant loading direction) with online acoustic emission (AE) monitoring were performed in order to validate the simulation results. AE monitoring was used to assess the onset of cracking from the existing pores. Therefore two AE sensors were clamped close to the edges of the test samples and the energy of located AE events between the AE sensors was measured during the entire test campaign. Figure 11 shows the energy of the located AE emission events as function of the nominal applied stress for the tension tests on three different samples with different pore contents and the derived damage initiation stresses.

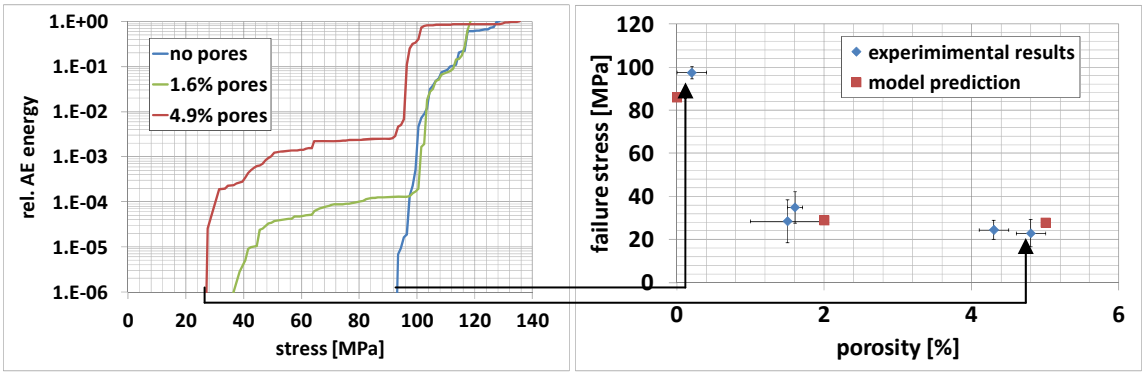

Figure 11. Energy of the located AE emission events as function of the nominal applied stress for the tension test on three different samples with different pore contents and the derived damage initiation stresses

As shown in Figure 11 the first indication of damage initiation starts at remarkable higher nominal stresses (around 92 MPa) in the nearly pore free sample compared to the sample with a pore content of around 4.9% (27 MPa) as predicted from the analyses. After the onset of the damages in the samples with the pores the damages seam to grow moderately indicated by the release of low average AE energy up to a stress level between 90 and 95 MPa (similar to initiation stress of the pore free sample). From this stress level the average AE energy is remarkable higher and comparable in all samples. This stress level indicates the rapid increase in crack density. When comparing the nominal stresses for damage onset from the tests with results from the analyses (see right side of Figure 11) the values can predicted with an average deviation of less than 10%.

6 Conclusion

Within this paper the authors have presented a simulation approach for the prediction of the production induced pore content and the damage onset in components made of NCF by vacuum infusion. Microstructural and chemical analyses of the produced panels have confirmed the predicted overall pore content but show limitation of the used software in the prediction of the actual pore location. Mechanical tension and 4 point bending with online AE monitoring have demonstrated the damage initiation stresses can be predicted with a deviation of less than 10%.

References

[1] Illston J.M., Domone P.L.J., "*Manufacturing techniques for polymer composites*, ISBN: 978-0-419-25860-5 (2001)
[2] Rangondet A.: *Experimental Characterisation of the Vacuum Infusion Process*, Thesis University of Nottingham (2005)
[3] Mattsson D.: *Mechanical Performance of NCF composites*, ISSN: 1402-1544 (2005)
[4] Puck A.: *Festigkeitsanalyse von Faser-Matrix-Laminaten: Modelle für die Praxis*, Hanser (1996)
[5] Förster R., Knappe W.: *Experimentelle und theoretische Untersuchungen zur Rissbildung an zweischichtigen Wickelrohren aus Glasfaser/Kunststoff unter Innendruck*, Kunststoffe **61**,8, 583-8 (1971)
[6] Foye R.L.: *The transverse poisson´s ratio of composites*, Jour. O. Comp. Mat., **Vol. 6**, 293-95 (1972)
[7] H. Schürmann: *Konstruieren mit Faser-Verbund-Werkstoffen*, Springer (2004)